

# PERFORMANCE ANALYSIS OF BALL BEARING CONTROLS FOR ENGINE OPERATING SYSTEM

Yang Kun, Tu Qiuye, Cai Yuanhu  
School of Power and Energy, Northwestern Polytechnical University

**Keywords:** *engine operating system, ball bearing controls, performance, numerical simulation*

## Abstract

Detailed experimental research had been implemented in order to obtain the performance of ball bearing control cables which is taken as the major transmission mechanism of engine operating system. Different configurations of ball bearing controls were tested to determine the parameters in the numerical model which is used to describe the ball bearing controls' performance. Displacement response and operating force response of the ball bearing controls have also been obtained from the experimental dynamic data. A numerical simulation platform was developed as a tool for engine operating system design.

## 1 Preview

The operating system is a connector between an aircraft and its engines and is responsible for the charge of pilot through a cockpit. Although FADEC play a very important role in the aircraft operating system, manual mechanical steering system is still widely used in some of the low-speed and transport aircraft for its simple structure and reliable operation.

For earlier transmission mechanism, the operating force can only be transmitted via tension. So it is necessary to constitute a loop with two cables running by turns for both pulling and dragging. This configuration was abandoned due to its disadvantages such as large space occupation, high installation complexity, low reliability, etc.

In 1990, Yoshiaki Ohoka patented a cable with ball bearing control. As a kind of remote

control products, ball bearing control cables (Fig. 1) are different from the ordinary cables. These controls are self-contained action/reaction systems and consist of an inner race (core) held between two outer races by a series of balls, all contained in a flexible metal casing of high radial rigidity and strength. The core is the active member that transmits linear motion, while the fixed race transmits the reaction to the primary end fitting mounting points. The balls are positioned by a ball retainer with no possibility of disengagement, allowing the control to transmit the input force with maximum accuracy and minimum friction loss [1].

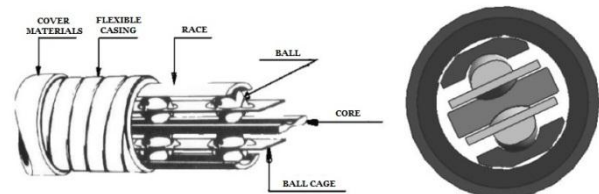


Fig. 1 Structure of Ball Bearing Controls

This ball bearing control cable has many advantages: easy to install, transmit tension and pressure in one cable, provides very precise movement with efficiencies between 85 percent and 95 percent regardless of control length, load, or configuration, and it also has high reliability and long service life span. Currently, ball bearing control cables has been widely applied in various fields, such as ships, trains, construction vehicles and aircraft.

This paper tested different construction of engine operating systems built by ball bearing control cables, in order to acquire the static performance and dynamic performance of the cable. Based on the test data, the static

performance of cables was fitted to optimize the engine operating system design, and the dynamic performance was also fitted to estimate the response from the throttle lever to the engine.

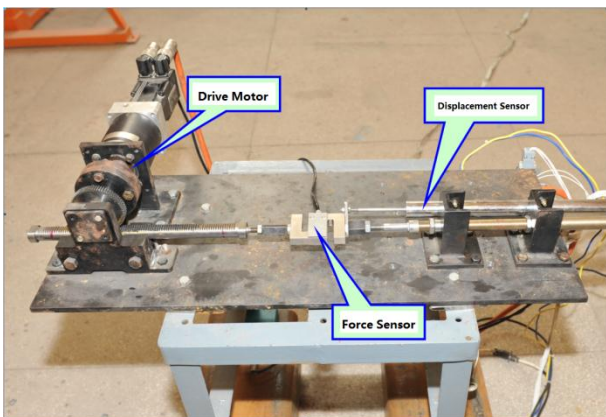
## 2 Tests and Data Analysis

As the connection mechanisms between the throttle lever and the engine, the performance parameters of the ball bearing controls consist of friction, operating force, backlash, and efficiency.

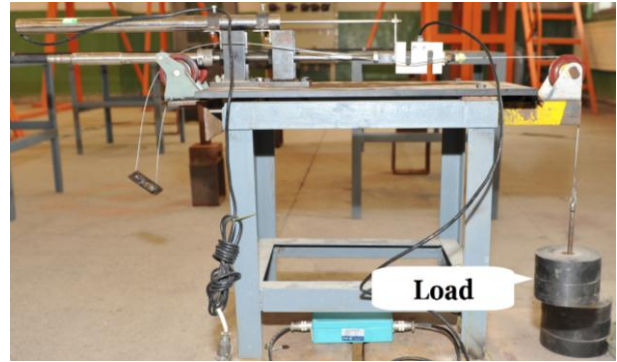


Fig. 2 Test of Ball Bearing Control Cable

In order to acquire the assessments of those parameters, different configurations of ball bearing control cables were tested as shown in Fig. 2. A motor, which generated slow and uniform movement for the core, was set at the upstream of the cable as the operating force (Fig. 3). A force sensor was set between the motor and the core to measure the output of the operating force. And two displacement sensors were set in parallel with the cable at both upstream and downstream to measure the displacement of the core. Different weights were loaded as inputs at the downstream of the cable.



(Upstream)



(Downstream)

Fig. 3 Installation of Driving Motor, Loads and Sensors

The factors of cable configuration include the length, the number of connectors, bending angle, bending radius, and twisting angle. So the configurations of the test illustrated in Fig.4 should contain all the factors' influences to the cable performance.

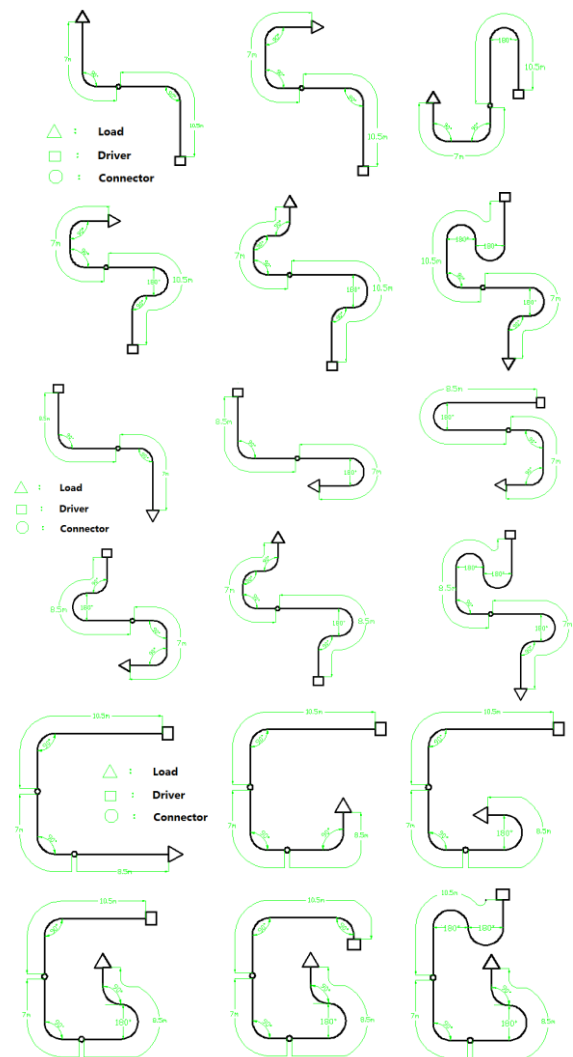


Fig. 4 Composed Configuration of Load, Bending and Connector

Test results show that friction is mainly affected by length (Fig. 5); operating force and backlash (Fig. 6) are mainly affected by load; bending angle has no significant impact on friction and backlash (Fig. 7) with the bending radius no less than 300 mm; slightly twisting angle has little impact on performance. The above conclusions were served as the basis for the empirical formulae of cable performance.

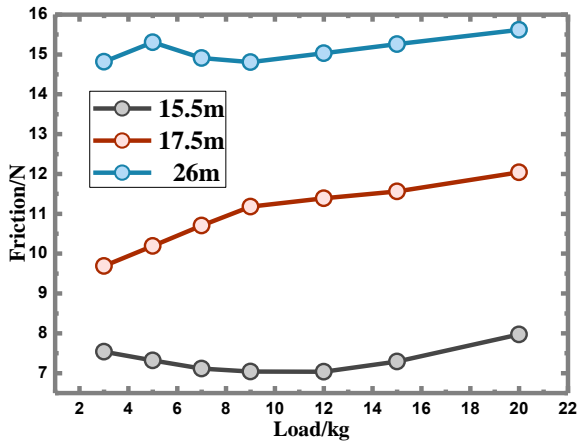


Fig. 5 The Variations of Friction with Load

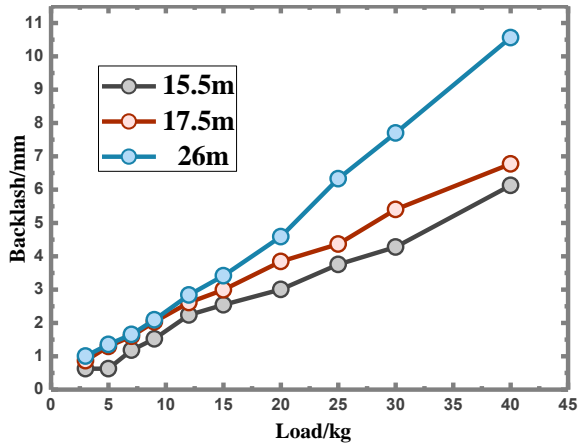


Fig. 6 The Variations of Backlash with Load

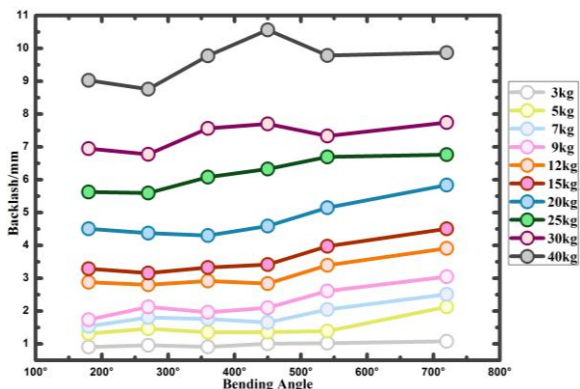


Fig. 7 The Variations of Backlash with Bending Angle

Fig. 6 also illustrates the high force transmission efficiency and control precision of the ball bearing control cable - even if under a larger load, 20kg for instance, the backlash of the cable can be controlled below 5mm.

### 3 Tests Curve Fitting

According to the test results, the friction is defined as a function of length, bending angle, and number of connection.

$$Fnlf = k_1 + k_2 \times L + k_3 \times \theta + k_4 \times J \quad (1)$$

The operating force is defined as a function of loading force, length, and bending angle for single ball bearing control. For the series connection of ball bearing controls, the operating force of downstream cable near the loads is taken as the input of loading force to calculate the operating force of the upstream cable.

$$F = k_5 + k_6 \times P + k_7 \times L + k_8 \times \theta \quad (2)$$

The backlash is defined as a function of operating force and bending angle for single ball bearing control. For the series connection of ball bearing controls, again, the operating force of downstream cable near the loads is taken as the input of loading force to calculate the backlash of the upstream cable.

$$B = k_9 + k_{10} \times F \times L + k_{11} \times \theta \quad (3)$$

The efficiency is defined as a ratio of loading force by operating force.

$$E = \frac{P}{F} \times 100\% \quad (4)$$

The coefficients from  $k_1$  to  $k_{11}$  can be calculated by solving the over-determined equations, since the number of test data is far more than the number of coefficients. Suppose there are  $m$  sets of test data and  $n$  underdetermined coefficients ( $m > n$ ), over-determined nonlinear equations can be obtained for the operating force and backlash, as shown in Equations (5).

$$\begin{cases} f_1(x_1, x_2, \dots, x_n) = 0 \\ f_2(x_1, x_2, \dots, x_n) = 0 \\ \dots\dots\dots \\ f_m(x_1, x_2, \dots, x_n) = 0 \end{cases} \quad (5)$$

The Taylor expansion is as following.

$$\begin{aligned} \frac{\partial f_1(x_1^0, x_2^0, \dots, x_n^0)}{\partial x_1} \Delta x_1 + \frac{\partial f_1(x_1^0, x_2^0, \dots, x_n^0)}{\partial x_2} \Delta x_2 + \dots + \frac{\partial f_1(x_1^0, x_2^0, \dots, x_n^0)}{\partial x_n} \Delta x_n &= -e_1 \\ \frac{\partial f_2(x_1^0, x_2^0, \dots, x_n^0)}{\partial x_1} \Delta x_1 + \frac{\partial f_2(x_1^0, x_2^0, \dots, x_n^0)}{\partial x_2} \Delta x_2 + \dots + \frac{\partial f_2(x_1^0, x_2^0, \dots, x_n^0)}{\partial x_n} \Delta x_n &= -e_2 \\ \dots\dots\dots \\ \frac{\partial f_m(x_1^0, x_2^0, \dots, x_n^0)}{\partial x_1} \Delta x_1 + \frac{\partial f_m(x_1^0, x_2^0, \dots, x_n^0)}{\partial x_2} \Delta x_2 + \dots + \frac{\partial f_m(x_1^0, x_2^0, \dots, x_n^0)}{\partial x_n} \Delta x_n &= -e_m \end{aligned} \quad (6)$$

Consequently, the matrix form:

$$A \cdot \Delta X = E \quad (7)$$

Where A is the coefficient matrix of (6), ΔX is the increment vector, and E the error vector. Equations (7) can be shifted to positive definite equations with both side pre-multiply the transposed matrix.

$$A^T A \cdot \Delta X = A^T E \quad (8)$$

Then the nonlinear equations (8) can be solved by Newton-Raphson method, and the iterative scheme is as follow:

$$X^{(n+1)} = X^{(n)} - [A^T A]^{-1} A^T E \quad (9)$$

### 4 Static Performance Analyses

Based on the empirical equations (1~4), it is convenient to develop a computer program to analyze the static performance of the 3D model, which have been built in CATIA, of the ball bearing control cables (Fig. 8).

The cable configuration can also be optimized with specified design boundary conditions. Generally, the boundary conditions include maximum cable backlash  $B_{max}$ , maximum loading  $P_{max}$  from the engine, minimum length  $L_{min}$  of straight segment, minimum radius  $r_{min}$  of bending, and minimum cable length  $L_{min}$ .

The backlash is often as the design goal of the cable configuration. It usually reaches maximum value  $B_{max}$  only when the loading from the engine reaches maximum  $P_{max}$ . So the

first constraint relationship between cable length and bending angle could be set up from the equation (2) and (3).

$$\theta = \frac{B_{max} - (k_1 + k_2 * L * (k_7 * P_{max} + k_8 + k_9 * L))}{k_2 * k_{10} * L + k_3} \quad (10)$$

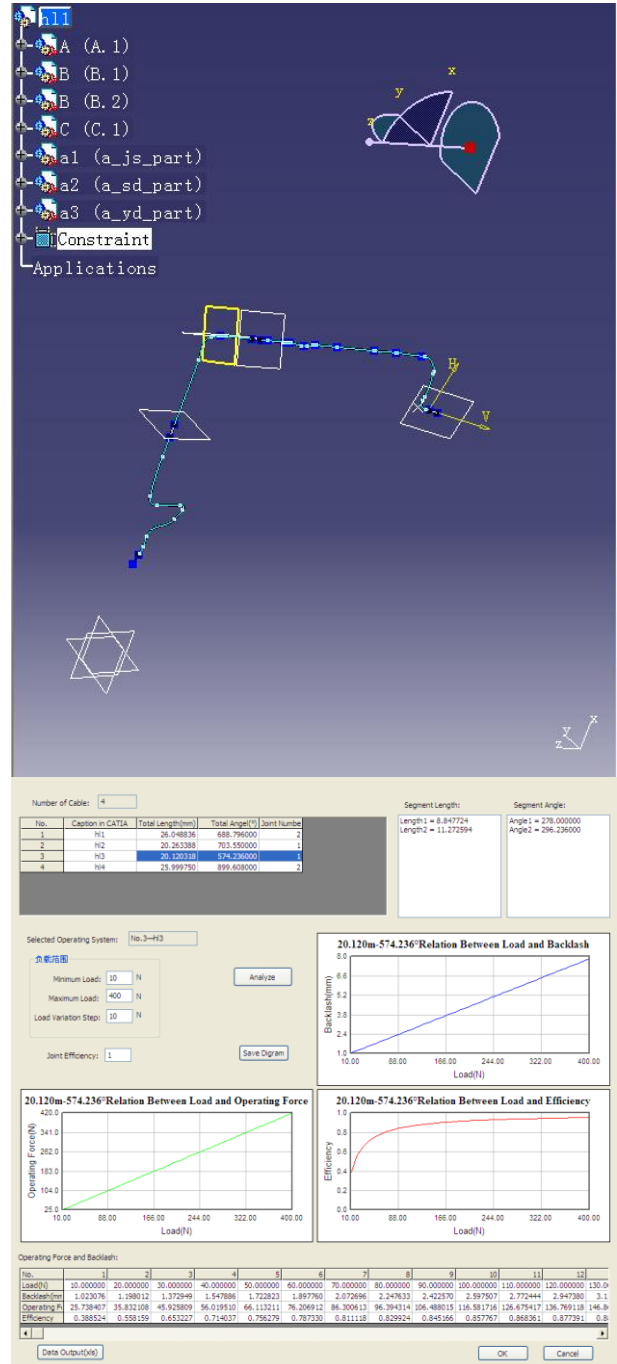


Fig. 8 Three-Dimensional Configuration Analysis

In the cable configuration, the straight parts and curved parts are usually distributed alternatively, because there must be a straight interval between two curved segment for normal



use, as shown in Fig. 9. Together with the line segment at both input and output, the number of straight segment are always one more than that of curly segments. For series connections, the joint must be placed between two line segment. Assuming that  $90^\circ$  as a bending unit, the second constraint relationship between cable length and bending angle could be set up with  $l_{min}$  and  $r_{min}$ .

$$L = \frac{\theta}{180} \pi r_{min} + \left( \frac{\theta}{90} + 1 \right) l_{min} + 2Jl_{min} \quad (11)$$

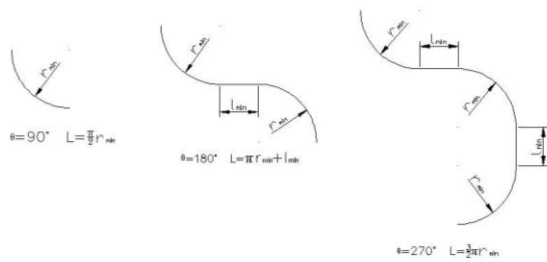


Fig. 9 Curly Segments and Line Segments Distribution

The solution area of the optimized layout parameters can be worked out with equations (10,11) and minimum cable length  $L_{min}$ , as shown in Fig.10. Within the solution area, all the configurations will satisfied the design goal of  $B_{max}$ .

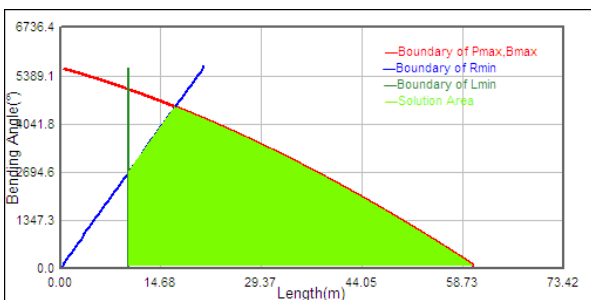


Fig. 10 Solution Area of the Optimized Layout Parameters

### 5 Dynamic Performance Analyses

Fig.11 illustrates the mechanical link of aircraft operating system. The mechanical throttle console is connected to transmission ratio conversion device in the nacelle by the ball bearing control cable. Among those components, the cable has obvious inertia phenomenon and response dead zone (backlash), so its dynamic performance should be analyzed. The other

parts are rigidly connected so that their dynamic response can be ignored.

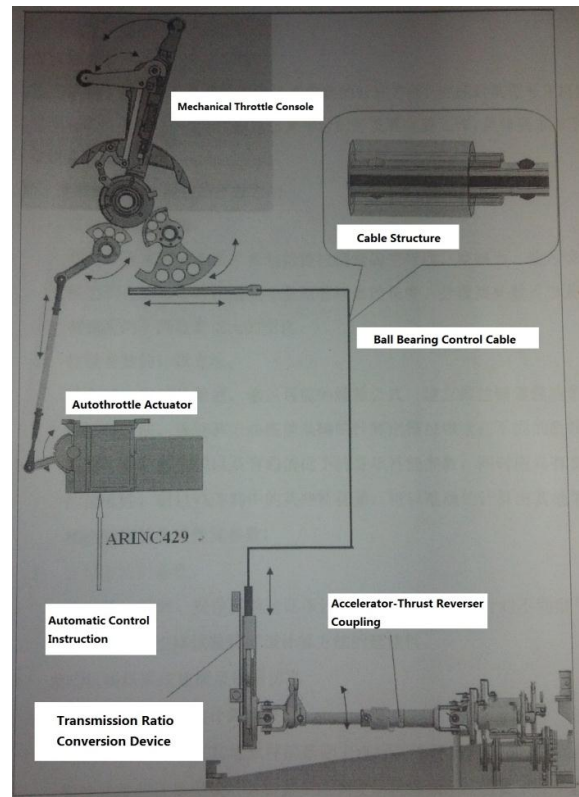


Fig. 11 Mechanical Engine Control System

The dynamic response of the ball bearing control cable includes the operating force response at the cable upstream and velocity response at the cable downstream. The simplified transfer functions were fitted from the test data as shown in Fig. 12 and Fig. 13. The operating force response is high order response, so there are some deviations for the simplified fitting curve. But the errors have no effects on the subsequent simulations.

The velocity response was obtained from the derivative of displacement response of test data. Obviously, the velocity response time is less than 0.3 seconds, and the operating force response time is less than 3 seconds.

Linking the velocity response of cable and the fuel pump response to the engine model, the total response was simulated as shown in Fig.14. Compared to the engine response time, the cable dynamic response time is so quick that its delay impact to the whole engine operating process can be ignored.

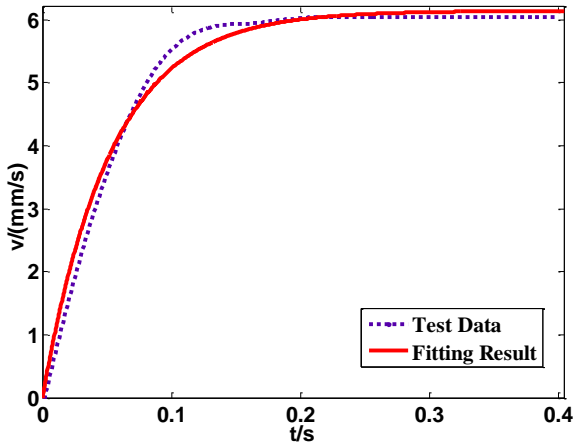


Fig. 12 Velocity Response

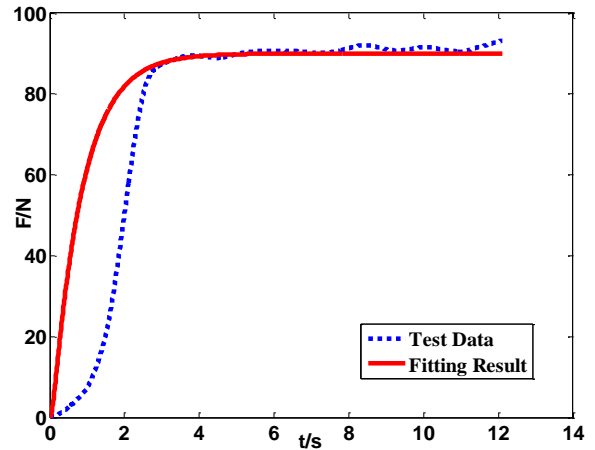


Fig. 13 Operating Force Response

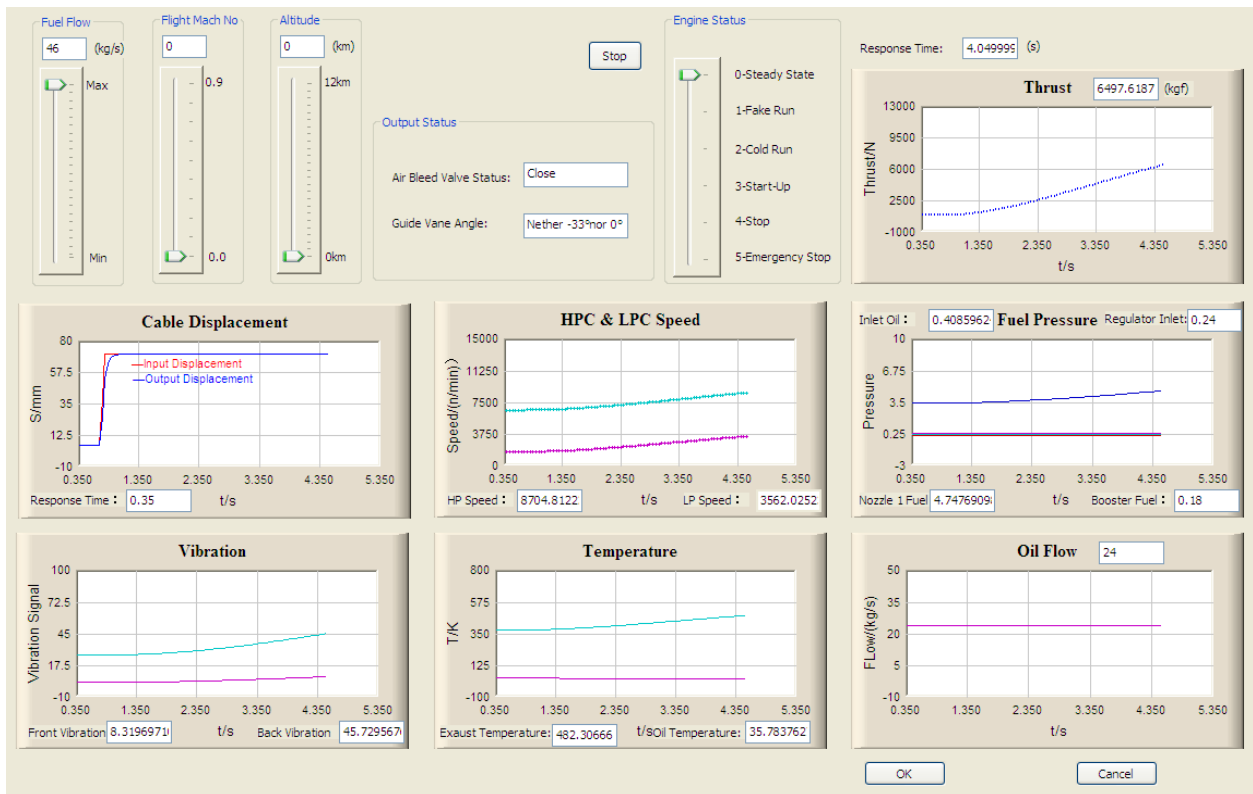


Fig. 14 Throttle Lever and Engine Simulation

## 6 Conclusions

Different configurations of transmission mechanism of the engine operating system have been tested. Tests results show that, among the performance parameters, friction is mainly affected by length, operating force and backlash are determined by load, while bending angle has no significant influence on performance. Due to the testing condition limitation, connection

impact to the performance cannot be analyzed independently.

According to the static analyses, the force transmission efficiency and control precision of the ball bearing control cable is quite high, and it can effectively meet the reliability requirements of the aero-engine manipulating system. The static performance curve fits given in this paper were the basis of the cable configuration optimization for the aircraft operating system.

The dynamic performance has been fitted to simulate the response from the throttle lever to the engine. Comparative result between the cable dynamic performance and the engine response outcome shows that the response of the cable is much faster than the engine, so the delay impact of the cable can be dismissed.

## **References**

- [1] Teleflex Incorporated, TELEFLEX DESIGN HANDBOOK.
- [2] Andrea Prencipe, Breadth and Depth of Technological Capabilities in CoPS: the Case of the Aircraft Engine Control System, Research Policy, 2000, Volume 29, Issues 7-8
- [3] Zhen Ren, System Identification and Control Design For Internal Combustion Engine Variable Valve Timing Systems, Degree of Doctor of Philosophy, Michigan State University, 2011
- [4] WESCON PRODUCTS COMPANY. PUSH-PULL CABLES CONTROL SYSTEMS. 2009.12
- [5] Makoto Shiota, Ikeda; Yukio Tomizawa, Hyogo; Yoshiaki Ohoka, Kobe. Control Cable. United States Patent (Patent Number: 4951523). Aug.28,1990

## **8 Contact Author Email Address**

jsyangkun@mail.nwpu.edu.cn

## **Copyright Statement**

The authors confirm that they, and/or their company or organization, hold copyright on all of the original material included in this paper. The authors also confirm that they have obtained permission, from the copyright holder of any third party material included in this paper, to publish it as part of their paper. The authors confirm that they give permission, or have obtained permission from the copyright holder of this paper, for the publication and distribution of this paper as part of the ICAS 2014 proceedings or as individual off-prints from the proceedings.